

Geomagnetic Dip Changes in the 1950 Eruption of Izu-Oshima Volcano, Central Japan : Magnetic Source Inversion Using Genetic Algorithm

Yoichi Sasai¹⁾

Abstract

Rikitake conducted repeat geomagnetic dip surveys during the first stage (Phase I activity : July-September, 1950) of the 1950 eruption of Izu-Oshima volcano, central Japan and found a large amount of changes in the dip. He devised a method to find an eccentric dipole from the surface magnetic observations and applied it to obtain a source for such magnetic changes as a thermally demagnetized sphere of radius 2.5 km at a depth of 5.5 km. His result bears an important suggestion to the magma sources of this volcano even for the 1986 eruptive activity. In 1986, the magma extruded in the fissure eruptions was strongly differentiated : Petrologists proposed that it came from a reservoir at a shallow depth which might have been formed by a past intrusive event. We investigate here if Rikitake's results are supportive of such an event. We reexamined the validity of his model by applying the present-day technique of magnetic source inversion, i.e. the genetic algorithm (GA). A constraint is that the source should be consistent with the magnetic structure beneath around Izu-Oshima volcano which has been clarified by the recent aeromagnetic surveys. A source for the observed magnetic changes was found as a flat, slightly inclined to the north, triaxial ellipsoid located shallower than 5 km depth. Implications of such a magma reservoir are discussed with special reference to the magma plumbing system of Izu-Oshima volcano.

1 Introduction

Izu-Oshima island is a basaltic volcano, about 110 km to the SSW of Tokyo, which is 15 km long (NS), 9 km wide (EW) and 758 m high. The volcano consists of a caldera of diameter 3 to 4.5 km, which bears a central cone called Miharayama. See Fig. 1. The last eruption occurred in November, 1986. It began with the summit eruption (phase I), followed by the flank fissure eruption (phase II). In November, 1987, one year later, the magma remained in a lava pond at the top of the central

cone drained back into depth and the volcano has been dormant since then.

Before the 1986-87 activity, the former eruption cycle started in 1950 with summit eruptions, which was followed by intermittent small-scale eruptions from the central cone until 1974. Fire fountaining eruptions began to occur at the summit of the central cone in July and continued until September, 1950. This period of the activity is called the phase I stage of the 1950-51 eruption. Lava flowed down the slope of the central cone onto the caldera floor during the phase I activity of the 1950 eruption.

1) Earthquake Prediction Research Center, Institute of Oceanic Research and Development, Tokai University, Orido, 3-20-1, Shimizu-ku, Shizuoka City, Shizuoka, 424-8610 Japan

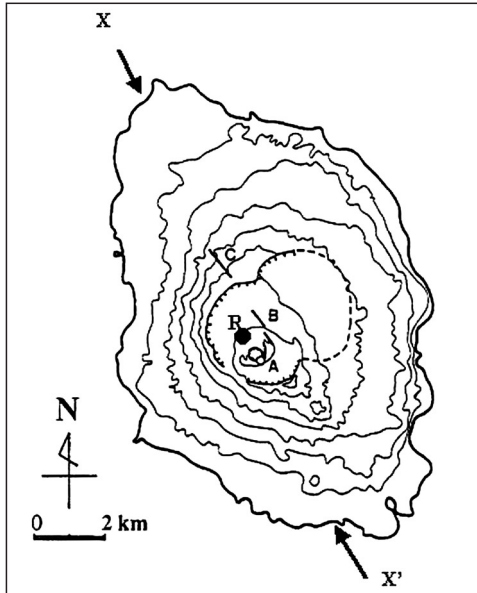


Fig. 1 Map of Izu-Oshima volcano. The hachured and dotted lines indicate the caldera rim. A is the central crater at the top of the central cone Miyarayama. B and C are the fissures which were formed during the 1986 eruption. R is the horizontal position of the center of the source sphere for the geomagnetic changes in the 1950 eruption by Rikitake (1951b). X and X' indicate both the ends of a line along which a vertical cross-section is shown in Fig. 6.

Just after the onset of the 1950 eruption, Rikitake (1951b) conducted geomagnetic dip survey over the volcano. He reoccupied the same benchmarks in September, 1950, when the summit eruption, or the phase I activity, suddenly stopped on September 23. Comparing both the surveys, he found a large amount of decrease in the geomagnetic dip up to 30 minutes of arc in the central part of the caldera. As a source for such magnetic changes, he ascribed it to a thermally demagnetized sphere of radius 2.5 km at a depth of 5.5 km beneath the volcano. The third survey was done in March 1951, by which no significant changes were detected in the geomagnetic field (Rikitake, 1951c).

Rikitake's (1951b) result was the second example of remarkable magnetic changes detected in the eruption of basaltic volcanoes in Japan, following the case of the 1940 eruption of Miyake-jima volcano, e.g.

Kato (1940), Takahasi and Hirano (1941a, b). In Izu-Oshima volcano, significant magnetic changes were observed associated with the intermittent summit eruptions (Yokoyama, 1969), which motivated to establish Nomashi magnetic observatory (ERI) on the island in 1960's. Continuous measurements of total intensity by proton precession magnetometers were maintained by the observatory as well as resistivity measurements on the central cone with DC controlled sources since 1970's (Yukutake *et al.*, 1987, 1990a).

Hence electromagnetic observations have been intensively conducted before, during and after the 1986-87 activity of Izu-Oshima volcano (Yukutake, 1990). Based on total intensity data at Nomashi magnetic observatory, Yukutake *et al.* (1990b) found a long-term (~ 10 years) anomalous decrease in the total intensity preceding the 1986 eruption. Also, changes in the total intensity were observed a few years (Yukutake *et al.*, 1990c) and several months (Sasai *et al.*, 1990) prior to the eruption. In particular, remarkable changes associated with the fissure eruption were interpreted as due to the piezomagnetic effect (Sasai, *et al.*, 1990). On the other hand, a large amount of changes in the total intensity after the eruptions were well explained in terms of the thermal demagnetization in the shallower part beneath the central cone (Hamano *et al.*, 1990).

Fujii *et al.* (1988) showed that the magma extruded from the fissures during the phase II activity in 1986 were much differentiated (SiO_2 contents : 54 ~ 57%). Aramaki and Fujii (1988) proposed that it came from a magma reservoir at some depth, which should have been formed by an intrusive event in the past. No evidence exists for such a hidden volcanic event. Taking notice of Rikitake's (1951b) results, we examined if the volcanomagnetic effect observed in 1950 was supportable of such an intrusive event. With the aid of recent knowledge on the magnetic structure of Izu-Oshima volcano, we attempt to present an alternative magnetic source, i.e. a triaxial ellipsoid.

2 Magnetic dip surveys and Rikitake's model

The eruption of Izu-Oshima volcano in 1950 started on July 16 and continued until September 23. Magnetic dip surveys were conducted by Rikitake (1951b) during the period of July 25-30 (Survey I) and during the period of September 25-30 (Survey II). Measurements were done using a miniature Earth-inductor developed by Rikitake (1951a).

He also presented an analytical formula for the magnetic field produced by a uniformly magnetized truncated circular cone (Rikitake, 1951b). He applied it to the results of the Survey I which covered Izu-Oshima island well, and obtained the average magnetization of the volcano as 0.03 emu (30 A/m). Comparing the two surveys, he found that the geomagnetic dip decreased as much as 30 minutes as shown in Fig. 2 (a).

Rikitake (1950a, b) devised a method to find an eccentric dipole below a surface on which any particular component of the magnetic field is known. As shown in Fig. 2 (b), Rikitake (1951b) obtained a magnetic dipole beneath the caldera at a depth

of 5.5 km. The north seeking end of the dipole was S42° E in the declination and -63° in the inclination, and its magnetic moment was estimated as 6.3×10^{14} emu (6.3×10^8 Am²). If we assume the average magnetization J_0 to be 30 A/m, the radius of the magnetized sphere is 1.7 km, while if we assume J_0 to be 10 A/m, its radius becomes 2.5 km.

3 Dipole source and its defects

Rikitake's (1951b) work was epoch-making in the history of volcanomagnetic study. According to his model, it is strongly suggested that a huge amount of magma intruded at depth during the phase I activity of the 1950 eruption. However, Rikitake's source model implies a huge magma reservoir with a radius 2.5 km, of which existence might be suspicious. Fortunately, Rikitake presented enough documents on his instrument and measurements. Based on these data, we can examine the validity of his model.

Measurement accuracy of the magnetometer

Rikitake (1951a) developed a miniature Earth-inductor type magnetometer convenient for field work. It was, in principle, a rotating solenoid coil to detect the direction of the ambient ge-omagnetic field : when the coil axis becomes parallel to the field, it produces no induced electric currents. The magnetometer was tested at TKB station near Kakioka magnetic observatory (KAK) for 24 hours from July 6 to 7, 1950.

Fig. 3 shows the comparison of geomagnetic dip between TKB and KAK, which is re-produced from the table in Rikitake (1951a). Scattering of measurements by the miniature magnetometer is relatively large as compared with the standard magnetogram at KAK, of which standard deviation amounts to 1.6 minutes of arc. In particular, the measurement error in the field conditions would be twice or more. Hence the accuracy of the simple differences between the two surveys can be estimated as 6 minutes of arc. This implies that we may allow the model fitness within the standard errors of 6 minutes for the discrepancy between the observation and the model estimate (O - C).

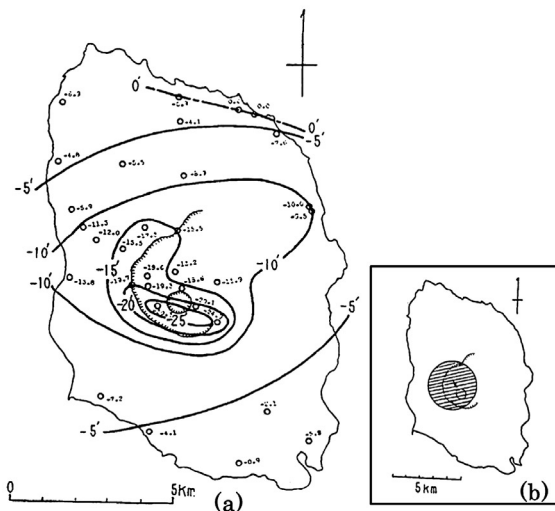


Fig. 2 (a) The distribution of geomagnetic dip changes between the Survey I and II. Unit in minutes of arc. After Rikitake (1951b). (b) The horizontal projection of the source sphere (radius 1.7 km) for geomagnetic dip changes when the magnetization is assumed as -30 A/m. After Rikitake (1951b).

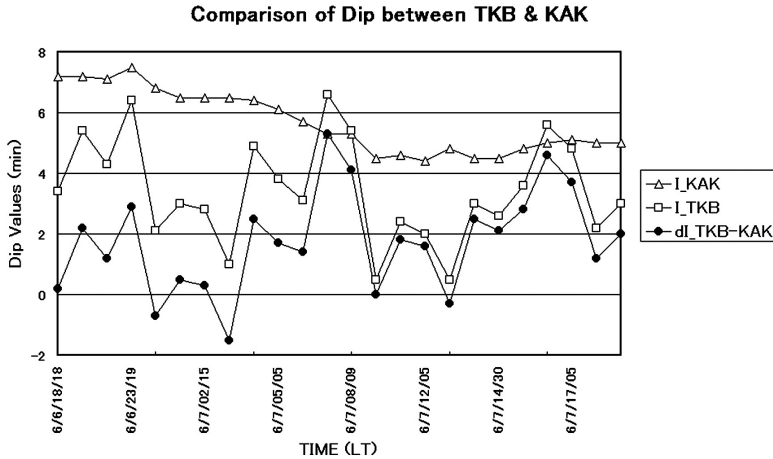


Fig. 3 Comparison of geomagnetic dip between TKB and KAK during the period from 18h June 6 to 18h June 7, 1950. After Rikitake (1951a). The standard deviation of the differences between TKB and KAK ($dI_{TKB-KAK}$) is 1.6 minutes of arc.

Reliability of the measurements

In 1936, Earthquake Research Institute had conducted magnetic survey with an absolute magnetometer of Japan Hydrographic Office type, of which measurement accuracy was 0.1 minutes. Rikitake (1951b) found some of the benchmarks in the previous survey, which revealed that the geomagnetic dip had increased by several minutes during the past 15 years (1936–1950). Such changes can be regarded as within the local differences of the secular change between Izu-Oshima and KAK. On the other hand, Rikitake (1951c) conducted the third repeat dip survey in March 1951 (Survey III). The differences between the Survey II and III were at most a few minutes. Hence the enormous changes in the geomagnetic dip took place only during the phase I activity of the 1950 eruption.

Average magnetization of Izu-Oshima volcano

Rikitake's (1951b) formula for the magnetic field of a truncated circular cone is a sophisticated one, which enabled him to accurately compute magnetic fields with the aid of a mathematical table for complete elliptic integrals. A circular cone is a more realistic shape for a volcano, as compared with the ones approximated by a sphere or a spheroid. Measurement on the ground was the only way to estimate the average magnetization of a volcano in

those days. However, we have so far had some good enough data for the magnetization of Izu-Oshima volcano by aeromagnetic surveys, e.g. Ueda *et al.* (1983), Nakatsuka *et al.* (1990), Ueda *et al.* (1990). They estimated the average magnetization of Izu-Oshima volcano as 10 A/m. Okubo (1984) obtained the depth of Curie point isotherm beneath around Izu-Oshima island as 5 km. In other words, if we seek to obtain a thermally demagnetized source, it must

lie between the depth from 0 to 5 km. The magnetic source obtained by Rikitake (1951b), i.e. a sphere of the radius 2.5 km (the magnetization assumed is -10 A/m) with its center at a depth of 5.5 km, is inadequate according to our recent knowledge on the magnetic structure beneath around Izu-Oshima volcano.

4 Source inversion for a magnetic dipole

Rikitake (1949a, b) proposed a method to find an eccentric dipole as a source for a given distribution of any particular magnetic component on a plane surface. In order to apply his method, we must interpolate the observed quantities obtained at various heights onto a certain horizontal plane above the observation sites, which is rather difficult to evaluate the errors. Rikitake (1951b) gave a table of observation sites (long., lat., height) together with the observed dip changes. We attempt here to find the best-fit dipole source to explain the observations using these data. Nakagawa *et al.* (1984) devised a grid search method to find the best-fit magnetic dipole to satisfy the observed changes in the geomagnetic total intensity after the 1983 eruption of Miyake-jima volcano. Although they did not give any details, I present here a brief description of the method.

Let us take the Cartesian coordinate system with x - axis positive to geographic north, y - axis to east and z - axis positive downward. The declination of the ambient geomagnetic field is taken as positive eastward. A magnetic dipole at $\mathbf{r}_0(x_0, y_0, z_0)$ makes a magnetic field $\Delta F(\Delta X, \Delta Y, \Delta Z)$ at $\mathbf{r}(x, y, z)$ as follows :

$$\begin{aligned} \Delta \mathbf{F} &= (\Delta X, \Delta Y, \Delta Z) = M_0 (\Delta f_x, \Delta f_y, \Delta f_z) \\ &= M_0 \left(\frac{A_x}{R^3} + \frac{3(x-x_0)A_R}{R^5}, \frac{A_y}{R^3} + \frac{3(y-y_0)A_R}{R^5}, \frac{A_z}{R^3} + \frac{3(z-z_0)A_R}{R^5} \right) \end{aligned} \quad (4)$$

where

$$R = |\mathbf{r} - \mathbf{r}_0| = \sqrt{(x-x_0)^2 + (y-y_0)^2 + (z-z_0)^2} \quad (2)$$

$$A_R = \mathbf{A} \cdot \mathbf{R} = A_x(x-x_0) + A_y(y-y_0) + A_z(z-z_0) \quad (3)$$

and M_0 is the magnetic moment of the dipole, while $\mathbf{A} = (A_x, A_y, A_z)$ is the direction cosine of the dipole. Assuming that the declination and inclination of the magnetization are D_M and I_M respectively, the direction cosine vector is given by

$$\mathbf{A} = (A_x, A_y, A_z) = (\cos I_M \cos D_M, \cos I_M \sin D_M, \sin I_M) \quad (4)$$

We denote the average declination, inclination and total intensity of the ambient magnetic field D_0 , I_0 and F_0 respectively. The direction cosine of the dip direction is given by

$$\mathbf{C} = (C_x, C_y, C_z) = (\sin I_0 \cos D_0, \sin I_0 \sin D_0, \cos I_0) \quad (5)$$

Hence the dip component is given by $F_I(\text{nT}) = \mathbf{C} \cdot \Delta \mathbf{F}$. When we represent the dip component in unit of minutes of arc, we have

$$F_I(\text{min}) = \frac{6.48 \times 10^5}{\pi F_0} \times \mathbf{C} \cdot \Delta \mathbf{F} \quad (6)$$

where F_0 is given in unit of nT.

Now we assume that magnetic changes are caused by the thermal demagnetization. Let us first try to find the best-fit magnetic dipole or a spherical source. Substituting $D_M = \pi - D_0$ and $I_M = \pi - I_0$, we can calculate $F_I(\text{min})$ at i -th observation point \mathbf{r}_i with only one unknown parameter M_0 once the position of the dipole \mathbf{r}_0 is specified :

$$F_I^C(i) = M_0 f_i(x_i, y_i, z_i) \quad (7)$$

in which f_i is computed via (1) and (7). We obtain M_0 which minimizes the following squared sum by the least square method,

$$S = \sum_{i=1}^N \{O_i - F_I^C(i)\}^2 \quad (8)$$

where N is the total number of observation points. The minimum standard deviation $\hat{\sigma}(\mathbf{r}_0) = \sqrt{S/(N-1)}$ indicates the model fitness. Since the magnetic moment M_0 of a uniformly magnetized sphere of radius a whose magnetization is J_M is given by $M_0 = 4\pi/3 a^3 J_M$, we can obtain the radius of the sphere.

We specify the horizontal position of Rikitake's (1951) dipole source as R point, which is identified by the coordinates (34.72905° N, 139.39317° E). Let us consider the grid points centering around R within ± 3 km at every 0.1 km spacing on a horizontal plane. In the following, we assume that $z = 0$ plane is located at the sea level. We also suppose grid points at every 0.1 km spacing from $z = 0$ to 10 km along a vertical axis centered at each horizontal grid point. At every $61 \times 61 \times 101$ points, we assume that each point is the position of a dipole and search for M_0 to minimize S . Thus we can find the best-fit dipole source for the observed dip changes between the two surveys in 1950. Table 1 shows the position of the best-fit dipole, together with the magnetic moment, its corresponding radius of the source sphere and the standard deviation of the model fitness. Also given in Table 1 are these parameters for Rikitake's (1951) original model. In Fig. 4 is shown the comparison of the model fitness between Rikitake's model and ours.

We notice in Fig. 4 that there are at least two distinct points which largely deviate from the best-fit line. We must take into account that some of the survey points were surrounded by lava flow during the period between the 1st and 2nd survey. Actually, the point which showed the maximum dip change was located close to the lava flow, and finally buried with lava at the time of the 3rd survey. Another anomalous point is located at the top of a sharp cliff of the caldera wall, where magnetic field gradient should be extremely high. We may exclude these

two points from input data for the source inversion. We tried again the dipole source inversion after removing the two points. The number of the survey points reduced from 31 to 29. However, the source position and its magnetic moment, i.e. the size of the sphere, were nearly the same as those in Table 1.

Although our model shows better fitness than Rikitake's, both the center position and the size of the source sphere are nearly the same as compared with each other. As we have discussed in the previous section, a thermally demagnetized spherical source largely protrudes out of the magnetic layer beneath Izu-Oshima island. One of the reasons for such a large demagnetized sphere is that the observed dip changes were negative almost everywhere which lacks the positive area. A deep spherical source does produce positive areas but somewhere outside Izu-Oshima island. The alternatives are ellipsoidal sources which could be included in the magnetized layer.

Table 1 Parameters for demagnetized dipole sources. The horizontal distance (x_0, y_0) is measured from R point. Results for (1) and (2) are obtained by using all the data points and those except two anomalous points, respectively.

Model	x_0 (km)	y_0 (km)	z_0 (km)	m_0 (Am ²)	a (km)	$\hat{\sigma}$ (min)
Rikitake (1951b)	0.0	0.0	5.5	6.3×10^8	2.50	—
(1) 31 points	-1.0	0.4	6.3	6.7×10^8	2.52	3.7
(2) 29 points	-0.7	0.2	6.6	6.6×10^8	2.51	2.7

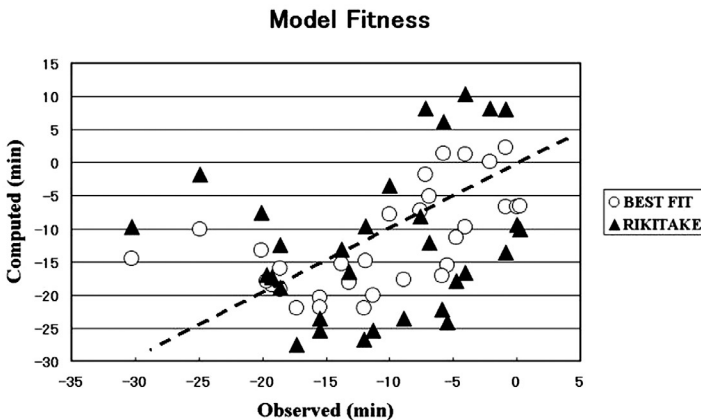


Fig. 4 Observed vs computed dip values at survey points for Rikitake's (1951b) model (solid triangles) and the best-fit model (hollow circles) by the present study.

5 Source inversion for a triaxial ellipsoid

In Appendix A we summarized the magnetic field produced by a triaxial ellipsoid. According to the formula, we can compute $\Delta F(\Delta X, \Delta Y, \Delta Z)$ at the survey points to find the dip value by eq. (6). The model parameters for a uniformly magnetized triaxial ellipsoid are twelve, i.e. (a) the coordinates of the ellipsoid center (x_e, y_e, z_e), (b) the lengths of three axes (a, b, c), (c) three angles to specify the attitude of the body (α, δ, γ), and the magnetization of the ellipsoid, i.e. the magnetization, declination and inclination (J_M, D_M, I_M). In the present case we assume that the body is thermally demagnetized, and hence the parameters (J_M, D_M, I_M) are known. We have nine unknown parameters to be determined.

In the recent decades, the Genetic Algorithm (GA) has been developed (Holland, 1975), and successfully applied to solve such non-linear geophysical source inversion problem with multiple parameters. In the volcano-EM studies, Currenti *et al.* (2005) first introduced GA techniques to find out the sources for the volcanomagnetic effect in the case of Mt. Etna and Miyake-jima volcano eruptions. Simple and effective FORTRAN subroutines for the GA inversion were published by Ishida *et al.* (1997), which are utilized in this study. Details of their applications will be given elsewhere.

However, we need a special consideration in applying the formulas for the magnetic field of a triaxial ellipsoid in Appendix A to GA inversion. The formulas begin with an assumption that $a > b > c$, and each attitude angle α, β or γ is defined with respect to three axes of the ellipsoid. The values

a , b and c should not be specified freely regardless of their order of length. On the other hand, each model parameter can be chosen arbitrarily at each step of GA inversion. Hence we introduce new parameters x_b and x_c , so that the axis length is given by $b = ax_b$ and $c = bx_c = ax_b x_c$, in which the intervals of the parameter space for x_b and x_c are limited as $0 < x_b < 1$ and $0 < x_c < 1$, respectively. The order of length values a , b and c is automatically satisfied as $a > b > c$.

Here we show the outline of the inversion procedure.

- 1) We consider grid points at every 0.1 km spacing, centered at R point horizontally within ± 1.5 km and vertically from 1 km to 3 km below the sea level. We assume that each grid point is the center of the ellipsoid.
- 2) Unknown parameters are lengths of three axes (a , b , c) and angles of attitude of the ellipsoid (α , δ , γ). Actually, we search for unknowns of x_b and x_c instead of b and c . We subdivide the parameter space into equal 256 cells for $0 < a \leq 3$ km, $0 < x_b \leq 1$, $0 < x_c \leq 1$, $0^\circ \leq \alpha \leq 360^\circ$, $0^\circ \leq \delta \leq 90^\circ$, and $-90^\circ \leq \gamma \leq 90^\circ$, respectively. We also impose a constraint that $H - z_e > a \sin \delta$ and $z_e > a \sin \delta$ (H is the Curie depth, specified as 5 km), which implies that the ellipsoid is included within the magnetized layer.
- 3) We compute the geomagnetic dip with each combination of (a , b , c , α , δ , γ). With the aid of GA, we search for the best fit model to

minimize the squared sum of the residuals S in eq. (8) at each grid point.

- 4) Comparing the minimum residuals at every grid points, we can find the best-fit position for the ellipsoid center as well as its parameters.

In Table 2 are shown the center position, shape and attitude parameters for the best-fit ellipsoid. The distribution of geomagnetic dip due to this model is shown at a height of 700 m above the sea level in Fig. 5. The standard deviation of the model fitness is 5.16 minutes, which is comparable with the standard error of the observations. The best-fit model is a flat, slightly inclined to the north, almost oblate ellipsoid, whose volume is 18.73 km^3 which is about a quarter of the demagnetized spherical source of 65.44 km^3 .

Table 2 Parameters for the best-fit triaxial ellipsoid. The horizontal distance (x_e, y_e) is measured from R point.

x_e (km)	y_e (km)	z_e (km)	a (km)	b (km)	c (km)	α (deg)	δ (deg)	γ (deg)	$\hat{\sigma}$ (min)
-0.8	0.2	3.0	2.99	2.68	0.558	350	6.4	83	5.16

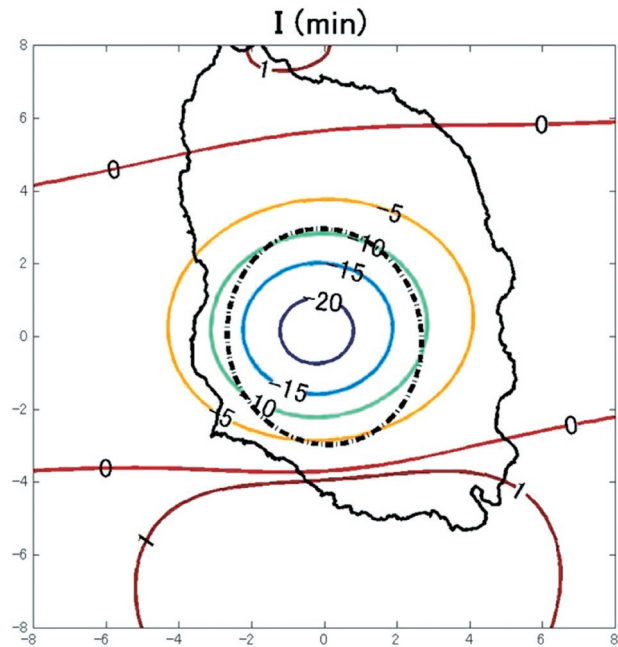


Fig. 5 The distribution of geomagnetic dip produced by a thermally demagnetized best-fit ellipsoid on a plane at a height of 700 m above the sea level. In unit of minutes of arc. Horizontal distance is given along both sides of the frame square. The dotted chain line indicates the horizontal projection of the ellipsoid.

6 Discussion

Fig. 6 shows a vertical cross-section of Izu-Oshima volcano along a line X-X' in Fig. 1, in which the position of the ellipsoidal source and Rikitake's spherical source are illustrated. As for Rikitake's model, we present two cross sections of the source sphere when we assume the average magnetization of the volcano as 30 A/m according to Rikitake's (1951b) analysis and as 10 A/m according to the recent result by Ueda *et al.* (1990). We notice that the ellipsoidal model is included within the magnetized layer, whose size is reasonably smaller than Rikitake's (1951) model. However, the volume of the ellipsoid is as much as 18.73 km^3 and we assume that it was completely replaced with magma.

During the magma intrusion event of the 1986 eruption (phase II activity), strong swarm

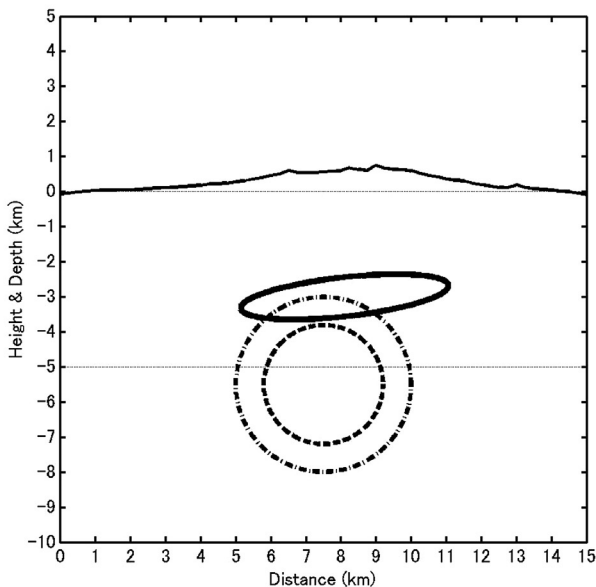


Fig. 6 A vertical cross-section of Izu-Oshima volcano along the line between X and X' in Fig. 1. The Curie point isotherm is shown by a straight dotted line at a depth of 5 km, while the surface topography is shown along the line X - X'. The thick solid line indicates the cross-section of the demagnetized ellipsoid, while the inner dashed line that of Rikitake's (1951b) spherical source for $J_0 = 30 \text{ A/m}$ and the outer chain line that for $J_0 = 10 \text{ A/m}$.

earthquakes took place associated with the dyke intrusion (Sawada *et al.*, 1988). However, no such strong earthquakes had ever been felt during the phase I activity (July to September, 1950) of the 1950 eruption. On the otherhand, people felt very slow and large shaking of the ground in those days (Miyazaki, T., *personal communication*). A possibility was that magma was filling any underground vacant space which caused such long-period volcanic tremors. Only when magma fills a vacant space, it does not result in magnetic changes. But suppose that the space was occupied by coarse and strongly magnetized scoria and that the materials were melted by magma, it could cause large magnetic changes. Actually, the scoria ejected in the 1986 eruption had an intense magnetization of 20 to 30 A/m, which had small density owing to vesiculation (Hamano *et al.*, 1990). We may imagine that there exists some vacant space in the shallow part of Izu-Oshima volcano and that magma fills the space during every eruptions but it drains back to depth after the eruptive activities. Note that the ellipsoidal source indicates an approximate shape of the vacant space and such space should be sustained by stiff framework of columns and crossbeams against the collapse, which has been usually considered as the structure for a 'magma reservoir' in volcanology (e.g. Fiske and Kinoshita, 1969). Similarly, the edifice of Miyake-jima volcano consists of stiff rocks with some vacant space as revealed by the formation process of a new caldera in its 2000 eruption (Nakada *et al.*, 2003).

The horizontal position of the center of a spherical source determined by Rikitake (1951b), i.e. R point in Fig. 1, roughly coincides with that of the B fissure in the phase II activity of the 1986 eruption. Moreover, the magma from the B fissure was surmised to have risen from a depth more than 5 km (e.g. Sawada *et al.*, 1988). The spherical source with its center at a depth of 5.5 km could be a good candidate for an isolated magma reservoir which should have been formed in the past intrusive activity, but only except for the reason that the

thermal demagnetization could not have taken place at such a depth deeper than 5 km. What does the shallow ellipsoidal source determined by the present analysis mean? After the 1950 eruption, intermittent eruptions occurred from the summit crater, which accompanied substantial amount of geomagnetic changes, in particular in the declination (Yokoyama, 1969). Such intermediate-scale eruptions were supposed to have been caused by vesiculation of volatiles within cooling magma remained in a shallow magma pocket. The ellipsoidal source in Fig. 6 may represent the formation of such a magma pocket.

After the 1986 eruption of Izu-Oshima volcano, a large amount of H₂O and SO₂ gas had been continuously emitted from the summit crater during the period from January 1988 to March 1990. The amount of degassed magma during the 27-month period was estimated as 2.6 × 10⁸ m³, which was 20 times larger than the volume of magma ejected during the 1986 summit eruption (Kazahaya *et al.*, 1994). As for Izu-Oshima volcano, a possibility is suggested by the present study that there exist magma pockets in the shallow part of the volcano and that at some eruption cycles magma fills the pockets and drains back after the eruptive activities as was the case of the 1950-1974 activity.

Acknowledgements

This study was done when I was at Disaster Prevention Division of Tokyo Metropolitan Government. I joined a workshop for study of Izu-Oshima volcano eruption held at JMA by the Coordinating Committee on the Prediction of Volcanic Eruption, in which the detailed process of the 1950 and 1986 eruptions of Izu-Oshima volcano was reexamined. I am greatly indebted to Dr Tsutomu Miyazaki, the former Disaster Prevention Specialist, who kindly provided me with valuable information on the 1950 eruption. I am thankful to Professor Omer Aydan, who critically read the manuscript and helped me improve it.

Appendix A : Magnetic field due to a uniformly magnetized triaxial ellipsoid

Let us take a Cartesian coordinate system (x, y, z), in which the center of an ellipsoid is located at its origin and the major, intermediate and minor axis are oriented in the x -, y - and z - direction respectively. We may call such a coordinate system which is fixed to the ellipsoidal body as the body coordinate. The basic equation for the triaxial ellipsoid is given by

$$\frac{x^2}{a^2} + \frac{y^2}{b^2} + \frac{z^2}{c^2} = 1 \quad (c^2 < b^2 < a^2) \quad (A.1)$$

The magnetic field produced by the uniformly magnetized ellipsoid is derived by Clark *et al.* (1986) as follows :

$$\begin{aligned} \frac{X_x}{2\pi abcJ_x} &= -A(\lambda) + \frac{2x^2}{g} \frac{1}{(a^2 + \lambda)^2} \frac{1}{\sqrt{\varphi(\lambda)}}, \\ \frac{Y_x}{2\pi abcJ_x} &= \frac{2xy}{g} \frac{1}{(a^2 + \lambda)(b^2 + \lambda)} \frac{1}{\sqrt{\varphi(\lambda)}}, \\ \frac{Z_x}{2\pi abcJ_x} &= \frac{2xz}{g} \frac{1}{(a^2 + \lambda)(c^2 + \lambda)} \frac{1}{\sqrt{\varphi(\lambda)}}, \\ \frac{X_y}{2\pi abcJ_y} &= \frac{Y_x}{2\pi abcJ_x}, \\ \frac{Y_y}{2\pi abcJ_y} &= -B(\lambda) + \frac{2y^2}{g} \frac{1}{(b^2 + \lambda)^2} \frac{1}{\sqrt{\varphi(\lambda)}}, \\ \frac{Z_y}{2\pi abcJ_y} &= \frac{2yz}{g} \frac{1}{(b^2 + \lambda)(c^2 + \lambda)} \frac{1}{\sqrt{\varphi(\lambda)}}, \\ \frac{X_z}{2\pi abcJ_z} &= \frac{Z_x}{2\pi abcJ_x}, \quad \frac{Y_z}{2\pi abcJ_z} = \frac{Z_y}{2\pi abcJ_y}, \\ \frac{Z_z}{2\pi abcJ_z} &= -C(\lambda) + \frac{2z^2}{g} \frac{1}{(c^2 + \lambda)^2} \frac{1}{\sqrt{\varphi(\lambda)}}, \end{aligned} \quad (A.2)$$

where

$$\begin{aligned} g &= \frac{x^2}{a^2 + \lambda} + \frac{y^2}{b^2 + \lambda} + \frac{z^2}{c^2 + \lambda}, \\ \varphi(\lambda) &= (a^2 + \lambda)(b^2 + \lambda)(c^2 + \lambda) \end{aligned} \quad (A.3)$$

and λ is the maximum root of the following cubic equation with respect to s :

$$\frac{x^2}{a^2 + s} + \frac{y^2}{b^2 + s} + \frac{z^2}{c^2 + s} - 1 = 0 \quad (A.4)$$

In the eqs. (A.2), $A(\lambda)$, $B(\lambda)$ and $C(\lambda)$ are defined as

$$A(\lambda) = \frac{2}{(a^2 - c^2)^{\frac{3}{2}} k^2} [F(k, \vartheta) - E(k, \vartheta)] \quad (A.5)$$

$$B(\lambda) = \frac{2}{(a^2 - c^2)^{\frac{3}{2}} k^2 k'^2} \left[E(k, \vartheta) - k'^2 F(k, \vartheta) - k^2 \frac{\sin \vartheta \cos \vartheta}{\sqrt{1 - k^2 \sin^2 \vartheta}} \right] \quad (\text{A.6})$$

$$C(\lambda) = \frac{2}{(a^2 - c^2)^{\frac{3}{2}} k'^2} \left[\frac{\sin \vartheta \sqrt{1 - k^2 \sin^2 \vartheta}}{\cos \vartheta} - E(k, \vartheta) \right] \quad (\text{A.7})$$

where ϑ , k and k' are given by

$$\sin \vartheta = \sqrt{(a^2 - c^2)/(a^2 + \lambda)} \quad (0 < \vartheta \leq \pi/2) \quad (\text{A.8})$$

$$k = \sqrt{(a^2 - b^2)/(a^2 - c^2)}, \text{ and } k' = \sqrt{1 - k^2} \quad (\text{A.9})$$

$F(k, \vartheta)$ and $E(k, \vartheta)$ are the incomplete elliptic integral of the first and second kind, respectively :

$$F(k, \vartheta) = \int_0^{\vartheta} \frac{d\theta}{\sqrt{1 - k^2 \sin^2 \theta}}, \quad (\text{A.10})$$

$$E(k, \vartheta) = \int_0^{\vartheta} \sqrt{1 - k^2 \sin^2 \theta} d\theta$$

With the aid of standard subroutines for the incomplete elliptic integrals and Cardano's formula for the cubic equation, we can easily compute the magnetic field components.

Let us consider an ellipsoid under the geographical coordinate system (x_0, y_0, z_0) , in which x_0 axis is oriented to the geographic north, y_0 axis to the

geographic east and z_0 axis positive downward. We assume that the center of an ellipsoid is located at $C(0, 0, h)$ as shown in Fig. A.1. Generally, the ellipsoid is inclined with respect to the horizontal $x_0 - y_0$ plane. The attitude of the ellipsoid is specified with three angles α , δ and γ . The downward major axis direction is called the plunge direction. The plunge direction is determined by two angles α and δ , where the major axis plunge azimuth α is measured clockwise from the positive x_0 direction ($0^\circ \leq \alpha \leq 360^\circ$), while the plunge δ is the angle between the horizontal plane and the downward major axis measured positive downward from $x_0 - y_0$ plane ($0^\circ \leq \delta \leq 90^\circ$). Then we define the intermediate axis direction as the angle γ between upward-directed intermediate axis and vertical plane containing major axis, positive clockwise looking along the x_0 axis ($-90^\circ \leq \gamma \leq 90^\circ$). See Fig. A.1.

In the body coordinate system fixed to the ellipsoidal axes, we consider mutually orthogonal unit vectors $\hat{\nu}_1, \hat{\nu}_2$ and $\hat{\nu}_3$ which are oriented in the x -, y - and z - direction respectively in eq. (A.1). Here we follow the definition of the body axes by Clark *et al.* (1986). Unit vectors $\hat{\nu}_j$ ($j = 1, 2, 3$) are given by

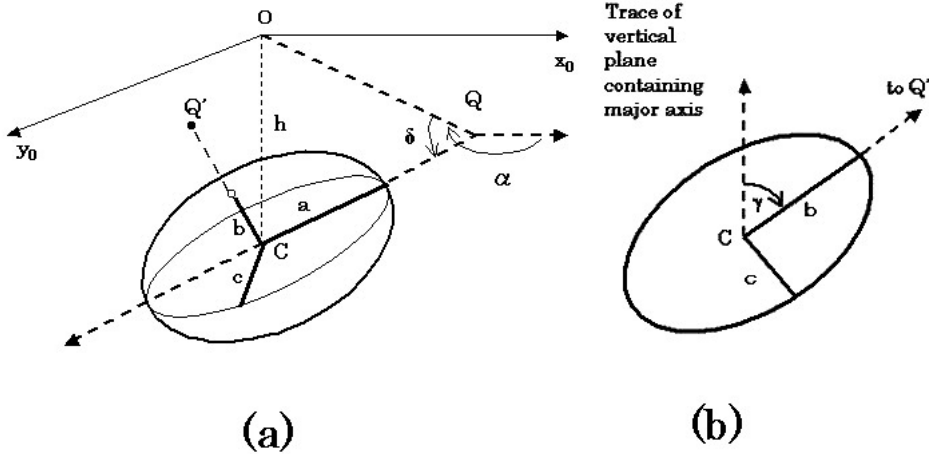


Fig.A.1. (a) A schematic representation of an inclined ellipsoid. C : center of ellipsoid. Q : intersection of extrapolated major (a) axis of ellipsoid with $x_0 - y_0$ plane. Q' : intersection of extrapolated intermediate (b) axis of ellipsoid with $x_0 - y_0$ plane. α : azimuth of plunge of major axis. δ : plunge of major axis. (b) The definition of angle γ , i.e. the angle between upward-directed intermediate axis and vertical plane containing major axis. The upward dotted arrow indicates trace of vertical plane containing major axis ($\triangle OCQ$ in (a)). This is not a vertical section but a section by an inclined plane dipping away from the viewer.

$$\begin{aligned} \hat{\nu}_1 &= (l_1, m_1, n_1) \\ l_1 &= -\cos \alpha \cos \delta, \\ m_1 &= -\sin \alpha \cos \delta, \\ n_1 &= -\sin \delta \end{aligned} \quad (\text{A.11a})$$

$$\begin{aligned} \hat{\nu}_2 &= (l_2, m_2, n_2) \\ l_2 &= \cos \alpha \cos \gamma \sin \delta + \sin \alpha \sin \gamma, \\ m_2 &= \sin \alpha \cos \gamma \sin \delta - \cos \alpha \sin \gamma, \\ n_2 &= -\cos \gamma \cos \delta \end{aligned} \quad (\text{A.11b})$$

$$\begin{aligned} \hat{\nu}_3 &= (l_3, m_3, n_3) \\ l_3 &= \sin \alpha \cos \gamma - \cos \alpha \sin \gamma \sin \delta, \\ m_3 &= -\cos \alpha \cos \gamma - \sin \alpha \sin \gamma \sin \delta, \\ n_3 &= \sin \gamma \cos \delta \end{aligned} \quad (\text{A.11c})$$

The body coordinate (x, y, z) is related to the geographical coordinate (x_0, y_0, z_0) as follows :

$$\begin{pmatrix} x \\ y \\ z \end{pmatrix} = \begin{pmatrix} l_1 & m_1 & n_1 \\ l_2 & m_2 & n_2 \\ l_3 & m_3 & n_3 \end{pmatrix} \begin{pmatrix} x_0 \\ y_0 \\ z_0 - h \end{pmatrix} \quad (\text{A.12})$$

Since the direction cosine of the magnetization is already given by A in eq. (4), the magnetization components in the body coordinate system or (J_x, J_y, J_z) in eq. (A.2) are expressed as :

$$\begin{aligned} (J_x, J_y, J_z) \\ (J_x, J_y, J_z) &= (\mathbf{J}_M \cdot \hat{\nu}_1, \mathbf{J}_M \cdot \hat{\nu}_2, \mathbf{J}_M \cdot \hat{\nu}_3) \end{aligned} \quad (\text{A.13})$$

where J_M is the uniform magnetization of the ellipsoid. Finally, we obtain the geographic north-, east- and downward component of the magnetic field as :

$$\begin{pmatrix} \Delta X \\ \Delta Y \\ \Delta Z \end{pmatrix} = \begin{pmatrix} l_1 & l_2 & l_3 \\ m_1 & m_2 & m_3 \\ n_1 & n_2 & n_3 \end{pmatrix} \begin{pmatrix} X_x + X_y + X_z \\ Y_x + Y_y + Y_z \\ Z_x + Z_y + Z_z \end{pmatrix} \quad (\text{A.14})$$

We can compute the magnetic field components at any arbitrary point (x_0, y_0, z_0) outside the ellipsoid via (A.14) and (A.2).

References

Aramaki, S., T. Fujii (1988) Petrological and geological model of the 1986-1987 eruption of Izu-Oshima Volcano, (*in Japanese with English abstract*), *Kazan (Bull. Volcanol. Soc. Japan)*, 33, S297-S306.

Clark, D. A., S. J. Saul, D. W. Emerson (1986) Magnetic and gravity anomalies of a triaxial ellipsoid, *Exploration Geophysics*, 17, 189-200.

Currenti, G., C. Del Negro, G. Nunnari (2005) Inverse modelling of volcanomagnetic fields using a genetic algorithm technique, *Geophys. J. Int.*, 163, 403-418.

Fiske, R. S., W. T. Kinoshita (1969) Inflation of Kilauea Volcano prior to its 1967-1968 eruption, *Science*, 65, 341-349.

Fujii, T., S. Aramaki, T. Kaneko, K. Ozawa, Y. Kawanabe, T. Fukuoka (1988) Petrology of the lavas and ejecta of the November, 1986 eruption of Izu-Oshima Volcano, (*in Japanese with English abstract*), *Kazan (Bull. Volcanol. Soc. Japan)*, 33, S234-S254.

Hamano, Y., H. Utada, T. Shimomura, Y. Tanaka, Y. Sasai, I. Nakagawa, Y. Yokoyama, M. Ohno, T. Yoshino, S. Koyama, T. Yukutake, H. Watanabe (1990) Geomagnetic variations observed after the 1986 eruption of Izu-Oshima Volcano, *J. Geomag. Geoelectr.*, 42, 319-335.

Holland, J. H. (1975) *Adaptation in natural and artificial system*, The MIT Press in Cambridge, Massachusetts, (2nd edition published in 1992).

Ishida, R., H. Murase, S. Koyama (1997) *Fundamental theories and application programs for genetic algorithms by personal computer*, (*in Japanese*), Morikita Shuppan, 101 pp.

Kato, Y. (1940) The changes in the earth's magnetic field accompanying the volcanic eruption of Miyake-zima, *Proc. Imp. Acad., Japan*, 16, 467-472.

Kazahaya, K., H. Shinohara, G. Saito (1994) Excessive degassing of Izu-Oshima volcano : magma convection in a conduit, *Bull. Volcanol.*, 56, 207-216.

Nakada, S., M. Nagai, T. Kaneko, A. Nozawa, K. Suzuki-Kamata, (2005) Chronology and products of the 2000 eruption of Miyakejima volcano, *Bull. Volcanol.*, 67, 205-218.

Nakagawa, I., Y. Sasai, H. Utada, Y. Ishikawa, S. Koyama, K. Oochi, T. Tokumoto (1984) Changes in total intensity of the geomagnetic field associated

- with the 1983 eruption of Miyake-jima volcano, (*in Japanese with English abstract*), *Kazan (Bull. Volcanol. Soc. Japan)*, 29, S101-S112.
- Nakatsuka, T., M. Makino, S. Okuma, T. Kaneko (1990) Aeromagnetic surveys over Izu-Oshima Volcano before and soon after the 1986 eruption, *J. Geomag. Geoelectr.*, 42, 337-353.
- Okubo, Y. (1984) Results of Curie depth analysis over the Japanese Islands, (*in Japanese*), *Chishitsu News (Geology News)*, No. 362, 12-17.
- Rikitake, T. (1950a) Magnetic anomalies and the corresponding magnetic centres I, *J. Geomag. Geoelectr.*, 2, 20-24.
- Rikitake, T. (1950b) Magnetic anomalies and the corresponding magnetic centres II, *J. Geomag. Geoelectr.*, 2, 25-28.
- Rikitake, T. (1951a) A miniature earth-inductor, *Bull. Earthq. Res. Inst., Univ. Tokyo*, 29, 147-153.
- Rikitake, T. (1951b) The distribution of magnetic dip in Ooshima (Oo-sima) Island and its change that accompanied the eruption of Volcano Mihara, *Bull. Earthq. Res. Inst., Univ. Tokyo*, 29, 161-181.
- Rikitake, T. (1951c) Changes in magnetic dip that accompanied the activities of Volcano Mihara (The 2nd report), *Bull. Earthq. Res. Inst., Univ. Tokyo*, 29, 499-502.
- Sasai, Y., T. Shimomura, Y. Hamano, H. Utada, T. Yoshino, S. Koyama, Y. Ishikawa, I. Nakagawa, Y. Yokoyama, M. Ohno, H. Watanabe, T. Yukutake, Y. Tanaka, T. Yamamoto, K. Nakaya, S. Tsunomura, F. Muromatsu, R. Murakami (1990) Volcanomagnetic effect observed during the 1986 eruption of Izu-Oshima Volcano, *J. Geomag. Geoelectr.*, 42, 291-317.
- Sawada, M., K. Kudo, M. Sakaue, H. Watanabe (1988) Strong seismic motion associated with the 1986 eruption of Izu-Oshima Volcano, (*in Japanese with English abstract*), *Kazan (Bull. Volcanol. Soc. Japan)*, 33, S102-S112.
- Takahasi, R., K. Hirano (1941a) Changes in the vertical intensity of geomagnetism that accompanied the eruption, *Bull. Earthq. Res. Inst., Univ. Tokyo*, 19, 82-103.
- Takahasi, R., K. Hirano (1941b) Changes in the vertical intensity of geomagnetism that accompanied the eruption, *Bull. Earthq. Res. Inst., Univ. Tokyo*, 19, 373-380.
- Ueda, Y., T. Tozaki, K. Onodera, T. Kaneko, S. Oshima (1983) Geomagnetic anomalies and magnetic structures of Quarternary volcanoes in Japan derived from aeromagnetic surveys, (*in Japanese with English abstract*), *Rept. Hydrogr. Res.*, No. 18, 37-64.
- Ueda, Y., H. Nakagawa, K. Kumagawa (1990) Aeromagnetic anomaly and derived structure of Izu Oshima Volcano after the eruption in November, 1986, *J. Geomag. Geoelectr.*, 42, 355-363.
- Yokoyama, I. (1969) Anomalous changes in geomagnetic field on Oshima Volcano related with its activities in the decade of 1950, *J. Phys. Earth*, 17, 69-76.
- Yukutake, T. (1990) An overview of the eruptions of Oshima Volcano, Izu, 1986-1987 from the geomagnetic and geoelectric standpoints, *J. Geomag. Geoelectr.*, 42, 141-150.
- Yukutake, T., T. Yoshino, H. Utada, H. Watanabe, Y. Hamano, Y. Sasai, T. Shimomura (1987) Changes in the electrical resistivity of the central cone, Miharayama, of Izu-Oshima Volcano, associated with its eruption in November, 1986, *Proc. Japan Acad.*, 63-B, 55-58.
- Yukutake, T., T. Yoshino, H. Utada, H. Watanabe, Y. Hamano, T. Shimomura (1990a) Changes in the electrical resistivity of the central cone, Miharayama, of Oshima Volcano observed by a direct current method, *J. Geomag. Geoelectr.*, 42, 151-168.
- Yukutake, T., H. Utada, T. Yoshino, E. Kimoto, K. Otani, T. Shimomura (1990b) Regional secular change in the geomagnetic field in the Oshima Island area during a tectonically active period, *J. Geomag. Geoelectr.*, 42, 257-275.
- Yukutake, T., H. Utada, T. Yoshino, H. Watanabe, Y. Hamano, Y. Sasai, E. Kimoto, K. Otani, T. Shimomura (1990c) Changes in the geomagnetic total intensity observed before the eruption of Oshima Volcano in 1986, *J. Geomag. Geoelectr.*, 42, 277-290.

伊豆大島火山 1950 年噴火に伴う地磁気伏角変化 — 遺伝的アルゴリズムを用いた磁気源インバージョン —

笹井 洋一¹⁾

要 旨

1950年伊豆大島噴火に際して、力武 (Rikitake, 1951) は 30分に及ぶ大きな地磁気伏角変化を観測した。この変化は山頂噴火の開始直後から溶岩流出が停止するまでの第一活動期にのみ検出された。力武は磁気異常解析から、中央火口丘の三原山北西部山麓の直下 5.5 km に、半径 2.5 km の球状熱消磁域が生じたことによる、と結論づけた。一方、1950年以降の噴火サイクルが終了した後、1986年に次の噴火サイクルが始まり、山頂噴火の直後に山腹割れ目噴火が発生した。割れ目噴火の地震経過と噴出物の岩石学的分析から、割れ目噴火のマグマは過去にある深さに貫入したまま地下に滞在し、結晶分化を遂げたと解釈された。1950年噴火時の地磁気変化はこのマグマ貫入事件に伴うものであった可能性がある。しかし 1970年代以降の航空磁気測量成果から、伊豆大島付近のキュリー点深度は 5 km であり、平均磁化は 10 A/m であるとされる。従って力武の求めた熱消磁領域は実際には発生し得ない。5 q より浅いという制約の下に観測された地磁気変化を説明するものとして、三軸不等楕円体の形状をした熱消磁領域の最適解を、遺伝的アルゴリズムを用いて求めた。得られた熱消磁領域は北に傾いた長径約 3 q の扁平な楕円体であり、1986年割れ目噴火の供給源とは考えられない。しかし 1950年噴火サイクルは 1974年まで中程度の噴火を繰り返しながら終息しており、この 1952-1974年後続活動のマグマ供給源であった可能性が高い。

1) 東海大学海洋研究所・地震予知研究センター

(2012年12月13日受付 / 2013年1月5日受理)